Displays 31 (2010) 191–195

Contents lists available at ScienceDirect

Displays

journal homepage: www.elsevier.com/locate/displa

An alternative bend-testing technique for a flexible indium tin oxide film

Yen-Liang Chen [a,b], Hung-Chih Hsieh [a], Wang-Tsung Wu [a], Bor-Jiunn Wen [b], Wei-Yao Chang [a], Der-Chin Su [a,*]

[a] Department of Photonics and Institute of Electro-Optical Engineering, National Chiao Tung University, 1001 Ta-Hsueh Road, Hsinchu 30010, Taiwan
[b] Center for Measurement Standards/Industrial Technology Research Institute (ITRI), Bldg. 16, 321, Kuang Fu Rd. Sec. 2, Hsinchu 30011, Taiwan

ARTICLE INFO

Article history:
Received 28 January 2010
Received in revised form 12 July 2010
Accepted 21 July 2010
Available online 24 July 2010

Keywords:
Indium tin oxide film
Bending test
Refractive index
Electro-optic modulation
Heterodyne interferometry

ABSTRACT

The two-dimensional refractive index distribution of a flexible indium tin oxide film deposited on a PET layer is measured before/after the bend-testing with an alternative technique based on Fresnel equations and the heterodyne interferometry. Their standard deviations are derived and they vary more obviously than the resistance variations measured in the conventional method. Hence the standard deviation of the refractive index can be used as the indicator to justify the durability of a flexible indium tin oxide film. The validity is demonstrated.

1. Introduction

Due to the high optical transmittance and the high conductivity of an indium tin oxide (ITO) film, it is widely used as the electrode for flat panel display devices, solar sells and organic light emitting diodes (OLED) [1]. In practice, the electronic patterns are printed on a thin ITO film deposited on a polyethylene terephthalate (PET) layer with laser patterning processes [2] to fabricate a flexible electronic substrate. The residual stress in part areas on the film caused by the temperature variation during the processes affects its quality and lifetime. The bending test can make the effect of the residual stress to be more obvious [3–7], so the resistance variation after definite bending cycles is always used as an indicator to justify its durability. However the resistance measurement is less sensitivity and the durability test becomes tedious due to its time-consuming bending cycles. To improve the sensitivity of this test, the two-dimensional microscopic refractive index distribution variations are observed instead of the conventional single-value resistance measurement.

Due to its photoelasticity [8], its refractive index is related with the residual stress. An alternative technique for measuring the two-dimensional refractive index distribution is presented based on Fresnel equations and the heterodyne interferometry. In this method, a collimated linearly/circularly polarized heterodyne light beam in turn enters a modified Twyman-Green interferometer, in which an ITO film is located in one arm for test. Two groups of full-field interference signals are taken by a fast CMOS camera. The sampling intensities recorded at each pixel are fitted to derive a sinusoidal signal, and its associated phase can be calculated. Then, substituting these two groups of phase distribution data into the special equations derived from Fresnel equations, its two-dimensional refractive index distribution and the standard deviation can be estimated. This film is tested before/after some different bending cycles. The standard deviation varies more obviously than the resistance variation measured with the conventional method. Hence the standard deviation of the two-dimensional refractive index distribution can be used as an indicator to justify its durability. The validity of this technique is demonstrated.

2. Principle

Fig. 1 shows a schematic diagram of this technique. For convenience, the $+z$-axis is chosen to be along the light propagation direction and the $+y$-axis is along the direction pointing out the paper plane. A light beam coming from a heterodyne light source [9] has a frequency difference f between the x- and the y-polarizations, and its Jones vector can be written as [10]

$$E_1 = \frac{1}{\sqrt{2}}\begin{pmatrix} e^{i\pi ft} \\ e^{-i\pi ft} \end{pmatrix}. \tag{1}$$

The light beam is expanded and collimated by a beam expander BE. It enters a modified Twyman-Green interferometer, which consists of a beam-splitter BS, a quarter-wave plates Q_2 with the fast axis at 45° with respect to the y-axis, a reference mirror M, a test sample S, an analyzer AN with the transmission axis at 0° with

* Corresponding author.
E-mail address: t7503@faculty.nctu.edu.tw (D.-C. Su).

0141-9382/$ - see front matter © 2010 Elsevier B.V. All rights reserved.
doi:10.1016/j.displa.2010.07.003

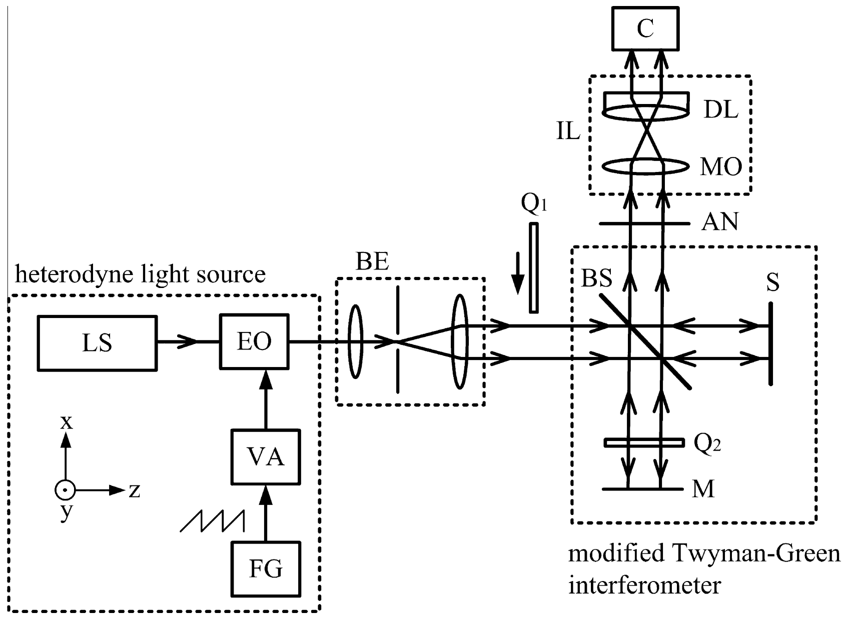

Fig. 1. Schematic diagram of this technique. LS: laser light source; EO: electro-optic modulator; FG: function generator; VA: voltage linear amplifier; BE: beam expander; Q: quarter-wave plate; BS: beam-splitter; M: mirror; S: sample; AN: analyzer; IL: imaging lens; MO: microscopic objective; DL: doublet; C: CMOS camera.

respect to the y-axis, an imaging lens IL, and a CMOS camera C. In this interferometer, two optical paths are (1) BS $\rightarrow$ Q_2 $\rightarrow$ M $\rightarrow$ Q_2 $\rightarrow$ BS $\rightarrow$ AN $\rightarrow$ IL $\rightarrow$ C (the reference beam), and (2) BS $\rightarrow$ S $\rightarrow$ BS $\rightarrow$ AN $\rightarrow$ IL $\rightarrow$ C (the test beam). For convenience, we firstly assume that the S is an isotropic material. So, their amplitudes can be derived and expressed as

$$\begin{aligned} E_{r1} &= (\mathrm{AN}(0^\circ)\cdot \mathrm{R_{BS}}\cdot \mathrm{Q}_2(-45^\circ)\cdot \mathrm{M}\cdot Q_2(45^\circ)\cdot E_1)\cdot e^{i\phi_{d1}} \\ &= \begin{pmatrix} 1 & 0 \\ 0 & 0 \end{pmatrix} \begin{pmatrix} e^{-i\phi_r/2} & 0 \\ 0 & e^{i\phi_r/2} \end{pmatrix} \frac{1}{\sqrt{2}} \begin{pmatrix} 1 & i \\ i & 1 \end{pmatrix} \begin{pmatrix} -r_m & 0 \\ 0 & r_m \end{pmatrix} \\ &\quad \times \frac{1}{\sqrt{2}} \begin{pmatrix} 1 & -i \\ -i & 1 \end{pmatrix} \frac{1}{\sqrt{2}} \begin{pmatrix} e^{i\pi ft} \\ e^{-i\pi ft} \end{pmatrix} e^{i\phi_{d1}} = \frac{ir_m e^{i(\phi_{d1}-\pi ft-\phi_r/2)}}{\sqrt{2}} \begin{pmatrix} 1 \\ 0 \end{pmatrix}, \end{aligned} \tag{2}$$

and

$$\begin{aligned} E_{t1} &= (\mathrm{AN}(0^\circ)\cdot \mathrm{S}\cdot \mathrm{R_{BS}}\cdot E_1)\cdot e^{i\phi_{d2}} \\ &= \begin{pmatrix} 1 & 0 \\ 0 & 0 \end{pmatrix} \begin{pmatrix} -r & 0 \\ 0 & r \end{pmatrix} \begin{pmatrix} e^{-i\phi_r/2} & 0 \\ 0 & e^{i\phi_r/2} \end{pmatrix} \frac{1}{\sqrt{2}} \begin{pmatrix} e^{i\pi ft} \\ e^{-i\pi ft} \end{pmatrix} e^{i\phi_{d2}} \\ &= -\frac{re^{i(\pi ft+\phi_{d2}-\phi_r/2)}}{\sqrt{2}} \begin{pmatrix} 1 \\ 0 \end{pmatrix}. \end{aligned} \tag{3}$$

Here, $\mathrm{R_{BS}}$, M and S are the reflection matrix of the BS, M and S; r_m and r are the reflection coefficients of the M and the S; ϕ_{d1} and ϕ_{d2} are the phase variations due to the optical path lengths of the reference and test beam, respectively. ϕ_r is the phase difference between the x- and y-polarizations coming from the reflection at BS. Thus, the interference signals recorded by the C can be written as

$$\begin{aligned} I_\mathrm{A} &= |E_{r1}+E_{t1}|^2 = I_{01} + \gamma_1 \cdot \cos(2\pi ft + \phi_1) \\ &= \frac{1}{2}\{r^2 + r_m^2 - 2rr_m \cos[2\pi ft + \frac{\pi}{2} - (\phi_{d1}-\phi_{d2})]\}, \end{aligned} \tag{4}$$

where I_{01}, and γ_1 and ϕ_1 are the mean intensity, the visibility and the phase of the interference signal, respectively. From Eq. (4), we have

$$\phi_1 = \frac{\pi}{2} - (\phi_{d1}-\phi_{d2}). \tag{5}$$

Secondly, the quarter-wave plate Q_1 with the fast axis at 45° to the y-axis is inserted into the optical setup as shown in Fig. 1 and the light amplitude becomes

$$\begin{aligned} E_2 &= \mathrm{Q}_1(45^\circ)\cdot E_1 = \frac{1}{2}\begin{pmatrix} 1 & -i \\ -i & 1 \end{pmatrix} \begin{pmatrix} e^{i\pi ft} \\ e^{-i\pi ft} \end{pmatrix} \\ &= \frac{1-i}{2}\begin{pmatrix} \cos(\pi ft)-\sin(\pi ft) \\ \cos(\pi ft)+\sin(\pi ft) \end{pmatrix} = \frac{1}{2}\begin{pmatrix} 1 \\ -i \end{pmatrix} e^{i\pi ft} + \frac{1}{2}\begin{pmatrix} -i \\ 1 \end{pmatrix} e^{-i\pi ft}. \end{aligned} \tag{6}$$

From Eq. (6), we can see that there is a frequency difference f between the right- and the left-circular polarizations, and it is a circularly polarized heterodyne light beam.

The amplitudes of the reference beam and the test beam can be derived as above and expressed as

$$\begin{aligned} E_{r2} &= (\mathrm{AN}(0^\circ)\cdot \mathrm{R_{BS}}\cdot \mathrm{Q}_2(-45^\circ)\cdot \mathrm{M}\cdot \mathrm{Q}_2(45^\circ)\cdot E_2)\cdot e^{i\phi_{d1}} \\ &= \begin{pmatrix} 1 & 0 \\ 0 & 0 \end{pmatrix} \begin{pmatrix} e^{-i\phi_r/2} & 0 \\ 0 & e^{i\phi_r/2} \end{pmatrix} \frac{1}{\sqrt{2}} \begin{pmatrix} 1 & i \\ i & 1 \end{pmatrix} \begin{pmatrix} -r_m & 0 \\ 0 & r_m \end{pmatrix} \\ &\quad \times \frac{1}{\sqrt{2}} \begin{pmatrix} 1 & -i \\ -i & 1 \end{pmatrix} \frac{1-i}{2} \begin{pmatrix} \cos(\pi ft)-\sin(\pi ft) \\ \cos(\pi ft)+\sin(\pi ft) \end{pmatrix} e^{i\phi_{d1}} \\ &= \frac{i+1}{2} r_m[\cos(\pi ft)+\sin(\pi ft)] e^{i(\phi_{d1}-\phi_r/2)} \begin{pmatrix} 1 \\ 0 \end{pmatrix}, \end{aligned} \tag{7}$$

and

$$\begin{aligned} E_{t2} &= (\mathrm{AN}(0^\circ)\cdot \mathrm{S}\cdot \mathrm{R_{BS}}\cdot E_2)\cdot e^{i\phi_{d2}} \\ &= \begin{pmatrix} 1 & 0 \\ 0 & 0 \end{pmatrix} \begin{pmatrix} -r & 0 \\ 0 & r \end{pmatrix} \begin{pmatrix} e^{-i\phi_r/2} & 0 \\ 0 & e^{i\phi_r/2} \end{pmatrix} \frac{1-i}{2} \begin{pmatrix} \cos(\pi ft)-\sin(\pi ft) \\ \cos(\pi ft)+\sin(\pi ft) \end{pmatrix} e^{i\phi_{d2}} \\ &= \frac{i-1}{2} r[\cos(\pi ft)-\sin(\pi ft)] e^{i(\phi_{d2}-\phi_r/2)} \begin{pmatrix} 1 \\ 0 \end{pmatrix}. \end{aligned} \tag{8}$$

Here the interference signals measured by the C can be written as

$$\begin{aligned} I_\mathrm{B} &= |E_{r2}+E_{t2}|^2 = I_{02} + \gamma_2 \cdot \cos(2\pi ft + \phi_2) \\ &= A\cdot \cos(2\pi ft) + B\cdot \sin(2\pi ft) + C, \end{aligned} \tag{9}$$